Chemical Composition of PM$_{10}$ at Urban Sites in Naples (Italy)

Paola Di Vaio [1], Elisa Magli [1], Francesco Barbato [1], Giuseppe Caliendo [1], Beatrice Cocozziello [2], Angela Corvino [1], Anna De Marco [3], Ferdinando Fiorino [1], Francesco Frecentese [1], Giuseppe Onorati [2], Irene Saccone [1], Vincenzo Santagada [1], Maria Eleonora Soggiu [4], Beatrice Severino [1] and Elisa Perissutti [1,*]

[1] Dipartimento di Farmacia, Università degli Studi di Napoli Federico II, Napoli 80131, Italy; paola.divaio@unina.it (P.D.V.); elisa.magli@unina.it (E.M.); francesco.barbato@unina.it (F.B.); caliendo@unina.it (G.C.); angela.corvino@unina.it (A.C.); fefiorin@unina.it (F.F.); frecente@unina.it (F.F.); irene.saccone@unina.it (I.S.); santagad@unina.it (V.S.); soggiu@iss.it (B.S.)

[2] Agenzia Regionale per la Protezione Ambientale in Campania, Napoli 80143, Italy; b.cocozziello@arpacampania.it (B.C.); g.onorati@arpacampania.it (G.O.)

[3] Dipartimento di Biologia, Università degli Studi di Napoli Federico II, Napoli 80126, Italy; ademarco@unina.it

[4] Reparto Igiene dell'Aria, Dipartimento Ambiente e Connessa Prevenzione Primaria, Istituto Superiore di Sanità 00161, Italy; soggiu@iss.it

* Correspondence: perissut@unina.it; Tel.: +39-081-678646

Abstract: Here, we report the chemical characterization and identification of the possible sources of particulate matter (fraction PM$_{10}$) at two different sites in Naples. PM$_{10}$ concentration and its chemical composition were studied using the crustal enrichment factor (EF) and principal component analysis (PCA). In all of the seasons, the PM10 levels, were significantly higher ($p < 0.01$) in the urban-traffic site (denominated NA02) than in the urban-background site (denominated NA01). In order to reconstruct the particle mass, the components were classified into seven classes as follows: mineral dust (MD), trace elements (TE), organic matter (OM), elemental carbon (EC), sea salt (SS), secondary inorganic aerosol (SIA) and undetermined parts (unknown (UNK)). According to the chemical mass closure obtained, the major contribution was OM, which was higher ($p < 0.01$) during summer than in other seasons. In both sites, a good correlation ($R^2 > 0.8$) was obtained between reconstructed mass and gravimetric mass. PCA analysis explained 76% and 79% of the variance in NA01 and NA02, respectively. The emission sources were the same for both sites; but, the location of the site, the different distances from the sources and the presence and absence of vegetation proved the different concentrations and compositions of PM$_{10}$.

Keywords: PM$_{10}$; chemical composition; enrichment factor; mass closure; principal component analysis

1. Introduction

Atmospheric particulate matter (PM) is composed of solid and/or liquid particles (except pure water) of different sizes and compositions, including organic and inorganic constituents formed by a large variety of mechanisms. The particulate can be associated with natural and anthropogenic sources [1]. PM can lead to cardiovascular and cerebrovascular diseases by the mechanisms of systemic inflammation, direct and indirect coagulation activation and direct translocation into systemic circulation [2]. PM determines oxidative stress and inflammation with anatomical and physiological remodeling of the lung causing respiratory morbidity and mortality [3].

Epidemiological studies have highlighted a correlation between the concentration/composition of the inhalable (particle size < 10 μm) and respirable (particle size < 2.5 μm) fractions (designated as PM_{10} and $PM_{2.5}$, respectively) and adverse respiratory effects. There is a great scientific interest in the chemical composition of atmospheric PM, which may depend on the source particles, the climate, the prevailing weather conditions and the chance for dispersion [4]. The legislation of PM levels (European Directive 2008/50/EC) sets limit values for the PM_{10} concentration: 40 μg·m^{-3} as the annual average and 50 μg·m^{-3} as the daily average, not to be exceeded more than 35 times in a year. The levels of specific PM components (metals, polycyclic aromatic hydrocarbons) are also regulated [5]. More recently, the International Agency for Research on Cancer has classified outdoor air pollution and, in particular, the particulate matter as carcinogenic to humans (Group 1) [6]. The components of air particles, including heavy metals, trace elements, organic compounds, ions, etc., may have damaging effects on human health, suggesting that the chemical composition of PM (which reflects differences in the source contributions) plays an important role in adverse biological responses [7].

In the scientific literature, several works are focused on the chemical composition and the impact of natural and anthropogenic sources on specific sites, investigating the role of specific emission sources. Terzi et al. (2010) [8] analyzed the concentration levels and the chemical composition of PM_{10} in the city of Thessaloniki (northern Greece), and the results demonstrated significant spatial and seasonal variations. Cesari et al. (2016) [9] evaluated the difference in the aerosol composition of $PM_{2.5}$ between a suburban and an urban site in southeastern Italy. $PM_{2.5}$ at the two sites were comparable, but the chemical composition and the contributions of the main sources were significantly different.

Therefore, the aim of this work was to characterize, as well as seasonal and spatial variations of the aerosol at two sites, an urban site and an urban background site, located in Naples, Italy. The chemical composition was used to calculate enrichment factors and to carry on statistical analysis with principal component analysis (PCA) to characterize the PM_{10} source types.

2. Experimental Section

2.1. Sampling Sites Description

The study was carried out in the urban area of Naples, from October 2012–July 2013. The Metropolitan city of Naples has the highest density of population in Italy and one of the highest in the EU. Its average density of population is more than 2500 inhabitants/km. The city is located in the "land of fires", a term used referring to an area of the Campania region that has a very high number of illegal waste burning practices [10]. Two sites were selected: the urban-background site (denominated NA01) and the urban-traffic site (denominated NA02). The NA01 site was a hypothetical background level (14°15′12.28″ E 40°51′44.79″ N), a green area close to a heavy traffic road (Tangenziale). The NA02 site was located in central Naples (14°15′5.54″ E 40°51′12.47″ N), at 2 km from the NA01 site and 1 km from the Naples harbor, and it is characterized by high traffic density. Furthermore, not far from the two sites are located small ceramic industries.

The Regional Environmental Protection Agency (signed ARPAC) has provided both sampling equipment. The climate of Naples is temperate (6–30 °C), strongly influenced by the sea breeze. The precipitation pattern is typical Mediterranean with a wet season in autumn-winter and a dry season in summer, while in spring, the monthly average rainfall is below 100 mm.

2.2. PM Sampling and Mass Measurement

PM_{10} samples were collected by two low volume PM_{10} samplers (Skypost, TCR Tecora) with a flow rate of 2.3 m^3·h^{-1} concurrently operating at each site (NA01 and NA02) during autumn (16 October–11 November 2012; 25 and 26 samples at NA01 and NA02, respectively), winter (1 March–15 March 2013; 15 samples at each site), spring (28 May–13 June 2013; 17 and 16 samples at NA01 and NA02, respectively) and summer (27 June–15 July 2013; 17 samples at each site). Twenty-four-hour samplings were performed according to EN-12341 [11]. PM_{10} was collected on high

purity quartz filters (Frisinette APS, 47 mm) pre-fired (500 °C for 4 h). Before and after sampling, filters were conditioned for 48 h at 20 ± 1 °C and 50% ± 5% relative humidity before weighing in a Sartorius SE 2-F microbalance. After weighing, the filters were preserved in Petri dishes in a cool (+4 °C) and dark place until analyses (for less than one week). Two percent of the samples were considered invalid due to technical problems with the samplers (i.e., short sampling times.)

2.3. Chemical Analysis

2.3.1. Metal Components

The analysis of the metals in PM_{10} was conducted according to the standard method for the measurements of Pb, Cd, As and Ni in the PM_{10} fraction of suspended particulate matter (EN 14902:2005) [12]. The samples were extracted by microwave-assisted digestion (Milestone MLS 1200 MEGA. FKV) in a PTFE vessel by adding HNO_3 (J.T. Baker 69%–70%) and H_2O_2 (Carlo Erba 30%) (5:2 *v/v*). The extracted solutions were then filtered through a 45-μm nylon filter for the removal of insoluble particles and were diluted with deionized water to 50 mL. The metals (Al, Sb, Ag, As, Ba, Cd, Cr, Fe, Mn, Mo, Ni, Pb, Cu, Se, V and Zn) in each sample were measured by inductively-coupled plasma mass spectrometry (ICP-MS Agilent 7500 ce), with a collision reaction cell operating in hydrogen mode to avoid matrix interferences.

Quantification was performed using a multi-element (Al, Sb, Ag, As, Ba, Cd, Cr, Fe, Mn, Mo, Ni, Pb, Cu, Se, V and Zn; Ultra Scientific) calibration standard method in the range of 0.10–250 μg/L (twelve-points calibration); 100 μL of a multi-elemental (250 μg/L Li, Sc, Rh, Y Ultra Scientific) solution were spiked as the internal standard into the standard solutions, blanks and extracted solutions. The correlation coefficients (R^2) for the calibration curves were all greater than 0.995.

The analytical method was checked for precision and accuracy. Limits of detection (LOD) were calculated based on 3SD/S (SD is the standard deviation of the response of seven replicate standard solution measurements, and S is the slope of the calibration graph). LODs of metals were in the range of 0.04–4.00 μg/L (Table 1). Blank filters were prepared and analyzed together with the samples, verifying that the metals' concentration values were under the LODs. The efficiency of the metals' analysis method was tested by using the spike method. In detail, 1.00 mL of the standard solutions (10 μg/L Ultra Scientific) was spiked on a quartz fiber filter. Recoveries of the metals from the spike method (*n* = 3) were in the range of 78%–96% (Table 1). For each batch of ten samples, a method blank and a spiked blank (internal standards spiked into solution) were analyzed. The coefficients of variation (CV) of the metals' concentration in duplicate samples were less than 7%.

Table 1. Limits of detection (LODs) of metals and recovery values.

Metals	LOD (μg/L)	Recovery ± SD%
Al	4.00	91 ± 6.0
Sb	0.10	78 ± 10
Ag	0.07	82 ± 6.0
As	0.10	85 ± 13
Ba	0.10	80 ± 6.0
Cd	0.04	87 ± 4.0
Cr	0.40	92 ± 5.0
Fe	3.00	89 ± 9.0
Mn	0.10	88 ± 12
Mo	0.06	91 ± 6.0
Ni	0.10	96 ± 7.0
Pb	0.12	92 ± 6.0
Cu	0.30	84 ± 10
Se	0.20	76 ± 11
V	0.12	85 ± 12
Zn	0.20	89 ± 7.0

2.3.2. Ionic Species

Another filter was cut into two equal parts by a ceramic lance, and the weights of both parts were then determined. Water-soluble ions (F^-, Cl^-, NO_3^-, SO_4^{2-}, Na^+, NH_4^+, K^+, Ca^{2+}) were analyzed in one part of the quartz filter. The samples were extracted four times with 10 mL of ultra-pure water (Milli-Q), renewing the water at each extraction, in an ultrasonic bath for 20 minutes, the necessary time for the complete recovery (78%–94%). Then, the solution was filtered through 0.45-μm cellulose acetate syringe filters (Albet Labscience, Dassel, Germany). Ions were determined applying ion chromatography (IC Metrohm 761). Cations were separated on a SUPP C4 cation column using a mixture of $HNO_3/(COOH)_2$ 2.00 mM. Anions were separated on a SUPP 5 anion column, preceded by a guard column of the same material, using a solution of $Na_2CO_3/NaHCO_3$ 3.20 mM; flow cell 1.00 mL·min^{-1} and 0.7 μS conductibility. Ions were identified by their elution/retention times and quantified by the conductivity peak areas.

Calibration curves for quantification were obtained using the internal standard method (six-point calibration) and were constructed in the following variable ranges: F^- (0.10–5.00 μg·mL^{-1}), NH_4^+, Na^+, K^+, Mg^{2+}, Ca^{2+}, Cl^-, NO_3^- and SO_4^{2-} (0.20–30.0 μg·mL^{-1}). The correlation coefficients (R^2) for the calibration curves were all greater than 0.998. The analytical method was checked for precision and accuracy. LODs of ionic species were in the range of 0.01–0.10 μg·mL^{-1} (Table 2). For each batch of ten samples, a method blank and a spiked blank (internal standards spiked into water) were analyzed. The coefficients of variation (CV) of ionic concentration in duplicate samples were less than 7%.

Table 2. Limits of detection (LODs) and recovery values.

Ionic Species	LOD (μg·mL^{-1})	Recovery $\pm$ SD%
F^-	0.01	88 ± 10
Cl^-	0.10	78 ± 9.0
NO_3^-	0.09	85 ± 11
SO_4^{2-}	0.10	87 ± 6.0
Na^+	0.08	84 ± 9.0
NH_4^+	0.06	94 ± 10
K^+	0.08	89 ± 7.0
Mg^{2+}	0.08	88 ± 10
Ca^{2+}	0.06	91 ± 9.0

2.3.3. Carbon Species (OC, EC and IC)

The second part of the quartz filter was used to determine the carbon species. Total carbon (TC) analysis was performed with an elemental analyzer (PE 2400 series II CHN analyzer. Perkin Elmer Cooperation, Waltham, MA, USA), according to the literature procedure [13], on two or more circular spots with a diameter of 0.95 cm, put into an apposite tin capsule (1 × 1 cm). The calibration curves for TC determination were obtained using potassium carbonate (Sigma-Aldrich, St. Louis, MO, USA) in the range 5.00–160 μgC. The determination of total inorganic carbon (IC) was executed using the same technique, after acidification of the filter spots with 1 M HCl and drying in a desiccator. The obtained value of carbon mass (C_1) was then subtracted from the amount of TC (IC = TC − C_1).

To determine the amount of the elemental carbon (EC), the filter spots, after acidification with 1 M HCl to eliminate IC, were positioned in an oven at 350 °C for 24 h.

The amount of organic carbon (OC) was determined by the difference (OC = TC − IC − EC). It is important to see that the distinction between EC and OC on the basis of thermal analysis is rather arbitrary and should be considered more an operative definition than a real chemical separation [14]. For each sample set, an unloaded filter piece of the same size was processed and analyzed and the blank values subtracted.

2.4. Statistical Analysis

One-way ANOVA, based on the F-test, detects significant differences among the sites and seasons. Moreover, the used Tukey test performed well in terms of both the accumulation of first order errors of the test and the test power [15–17]. Statistical analyses were performed by using the One-way Anova with post-hoc Tukey test [18]. Significance was evaluated as $p < 0.05$. Correlation analysis was performed by XLSTAT 2015.

3. Results and Discussion

3.1. PM$_{10}$ Mass Concentrations

The statistics of PM10 mass concentrations (minimum, maximum and mean) measured at the two sampling sites are reported in Table 3. In the urban-background site (NA01), the mean ± SD concentrations were comparable in each season, with mean values between 20.8 ± 4.00 and 26.6 ± 5.2 μg·m^{-3} in spring and autumn, respectively. The maximum concentration was registered during winter (54.8 μg·m^{-3}). In the urban-traffic site (NA02), the mean concentrations were higher ($p < 0.01$) than those of NA01 in each season; the mean values were between 27.1 ± 3.20 μg·m^{-3} in spring and 46.9 ± 7.8 μg·m^{-3} in autumn. The highest concentrations were observed in autumn with a maximum value of 68.7 μg·m^{-3} and eleven exceedances of the daily limit (national standard level for PM$_{10}$ corresponding to 50 μg·m^{-3}). The PM concentrations, often high during this period, were due to the increased emissions, associated with a meteorological period of high pressure days, which occurs as a consequence of the mid-latitude jet stream oscillations. In these days, the PBL (Planetary Boundary Layer) sometimes was below 100 m a.s.l., hindering air mixing.

Table 3. PM$_{10}$ mass concentration at two sites in μg·m^{-3} and the number of exceedances.

	Urban-Background Site (NA01)				Urban-Traffic Site (NA02)			
	Autumn	Winter	Spring	Summer	Autumn	Winter	Spring	Summer
Sample No.	25	15	17	17	26	15	16	17
Min	18.6	14.2	13.6	18.0	33.1	16.8	15.2	23.6
Max	46.7	54.8	29.8	45.2	68.7	59.2	31.6	46.4
Mean	26.6	25.8	20.8	26.6	46.9	38.3	27.1	35.0
No. exceeding	0	1	0	0	11	3	0	0

3.2. Metal Levels and Ionic Components

Summary data (mean, minimum and maximum) of 16 metals' concentrations determined in PM$_{10}$ air samples are reported in Tables 4 and 5 for the urban-background site (NA01) and the urban-traffic site (NA02), respectively. The metals represented, on average, 3%–4% of the PM$_{10}$ concentrations at both sites (NA01, NA02). Fe and Al were the most abundant among the metals at both sites and can be associated with soil resuspension and long-range transport of crustal dust [19]; followed by Cu and Zn, especially associated with traffic and combustion [20].

In autumn, Al, Fe, Cu and Mo showed great variation ($p < 0.01$) between the sites. Many elements (Cr, Cu, Fe, Al, Zn, Mn, Mo, Ag, Ba) demonstrated great variation ($p < 0.01$) between the four seasons at both sites. Particularly, Al, Fe, Mn and Mo showed significantly higher ($p < 0.01$) concentrations during autumn, while Ba and Ag exhibited a higher concentration, due to industrial and traffic emissions, during summer.

Furthermore, the concentrations of toxic metals (Pb, Ni, As and Cd), associated with PM$_{10}$ and classified by International Agency for Research on Cancer IARC as carcinogenic to humans (Group 1), did not exceed the EU's limits (500, 20, 6 and 5 ng·m^{-3}, respectively). Moreover, Cd and As were below the detection limit values.

In Tables 6 and 7 are reported the water-soluble ions' concentrations determined in PM$_{10}$ air samples for the urban-background site (NA01) and the urban-traffic site (NA02), respectively. At NA02,

many elements (F^-, Cl^-, K^+ SO_4^{2-}) showed significant ($p < 0.01$) differences between seasons; at NA01, other than the above-mentioned elements, also NO_3^- showed significant ($p < 0.01$) differences. In autumn, F^-, Cl^-, K^+ NO_3^- and SO_4^{2-} showed higher concentrations ($p < 0.01$) at NA02 than NA01; as the exception, Ca^{2+} and Mg^{2+} did not demonstrate significant seasonal variations at any of the sites, thus suggesting constant emissions throughout the year.

Table 4. Mean (min and max) metals' concentrations in PM_{10} in autumn, winter, spring and summer at the urban-background site (NA01) ($ng \cdot m^{-3}$).

Metals	Urban-Background Site (NA01)			
	Autumn	Winter	Spring	Summer
Al	400 (85.3–582)	311 (45.3–521)	285 (40.6–424)	280 (100–314)
Sb	26.1 (0.70–147)	–	3.90 (1.20–20.3)	–
Ag	7.00 (0.50–49.8)	11.8 (0.50–55.3)	13.2 (1.30–39.1)	24.3 (0.80–36.4)
As	–	–	–	–
Ba	26.5 (1.80–126)	25.4 (11.2–42.4)	38.6 (26.1–51.3)	55.7 (48.1–68.9)
Cd	–	–	–	–
Cr	10.6 (6.10–13.0)	32.7 (21.4–48.2)	56.0 (29.2–100)	45.8 (35.5–73.2)
Fe	469 (91.1–831)	327 (73.1–505)	289 (74.4–451)	287 (122–576)
Mn	23.0 (11.8–89.5)	14.1 (2.20–17.6)	8.40 (6.25–10.9)	10.4 (9.92–13.5)
Mo	2.84 (0.10–3.40)	0.70 (0.20–3.30)	0.50 (0.20–1.00)	0.70 (0.20–1.00)
Ni	7.40 (0.94–16.7)	3.48 (2.17–6.45)	7.43 (3.27–12.8)	3.91 (3.74–6.76)
Pb	11.2 (9.21–12.6)	3.17 (1.85–6.16)	12.0 (2.83–18.8)	6.11 (3.84–10.8)
Cu	22.6 (4.14–72.8)	30.7 (11.1–52.3)	47.3 (7.16–163)	70.5 (18.5–34.5)
Se	5.95 (0.22–25.3)	–	2.62 (0.22–38.7)	–
V	4.30 (0.32–27.7)	3.44 (0.10–6.33)	20.2 (4.12–59.2)	19.6 (5.12–49.7)
Zn	50.7 (21.7–285)	50.3 (10.3–107)	52.7 (0.70–158)	42.4 (32.2–64.9)

Table 5. Mean (min and max) metals concentrations in PM_{10} in autumn, winter, spring and summer at the urban-traffic site (NA02) ($ng \cdot m^{-3}$).

Metals	Urban-Traffic Site (NA02)			
	Autumn	Winter	Spring	Summer
Al	531 (55.6–687)	480 (53.8–636)	320 (45.5–568)	330 (112–559)
Sb	46.7 (4.90–107)	–	0.60 (0.2–1.30)	1.50 (0.20–12.4)
Ag	5.00 (0.50–26.6)	8.00 (0.40–44.3)	0.30 (0.10–3.60)	24.5 (0.20–12.4)
As	–	–	–	–
Ba	54.9 (7.77–146.3)	24.6 (11.0–45.6)	39.7 (26.6–47.2)	94.7 (48.2–198)
Cd	–	–	–	–
Cr	11.6 (5.72–18.9)	46.3 (27.4–105)	44.7 (24.1–146)	59.2 (0.20–91.6)
Fe	610 (221–1354)	492 (104–798)	320 (107–460)	331 (135–796)
Mn	30.1 (21.7–61.8)	24.8 (2.40–39.6)	9.10 (5.50–15.6)	10.6 (9.12–25.0)
Mo	4.60 (2.11–6.85)	3.71 (0.50–7.25)	0.30(0.200–3.90)	0.30 (0.10–2.60)
Ni	9.00 (1.00–24.9)	3.00 (1.00–9.70)	7.30 (2.00–36.1)	10.6 (1.64–5.34)
Pb	6.84 (0.20–17.2))	3.30 (0.600–7.14)	14.7 (2.00–31.2)	10.6 (1.66–85.3)
Cu	62.2 (6.34–207)	36.7 (11.1–112)	33.7 (15.1–70.0)	42.2 (14.9–82.7)
Se	4.14 (1.11–15.4)	0.44 (0.22–1.31)	–	1.35 (0.20–8.10)
V	3.60 (0.60–12.7)	8.12 (0.10–24.7)	19.9 (3.10–43.7)	47.6 (3.25–145)
Zn	45.1 (1.85–128)	62.9 (10.3–106)	33.3 (2.85–97.9)	83.7 (36.7–146)

Ionic soluble species were about 30% of PM_{10} concentrations. In particular, the sum of SO_4^{2-}, NO_3^- and NH_4^+ (SIA) represented about 20% of PM_{10} mass at both sites. This suggests that a significant part of aerosol is associated with the formation of secondary inorganic particles (SIA). The presence of dominant anions (SO_4^{2-} and NO_3^-) is due to the oxidations of NO_x and SO_2 (gaseous precursors) emitted from anthropogenic activities, particularly present in the urban ambient atmosphere. In both sites, during the summer, the higher concentrations ($p < 0.01$) of SO_4^{2-} suggested an additional photochemical formation, based on meteorological conditions [9], but it could also be related to the increase of ships docking in the port, which use sulfur-rich fuels. During the summer, the numbers of cruise ships, private and public ferries increase because Naples is a touristic location,

and the ferries link the city to the islands of Capri, Ischia, etc. Otherwise, the concentrations of nitrate were lowest in summer; this could be attributed to the low thermal stability of the nitrate in the hot season [21]. The greater concentrations of Na^+ and Cl^- ($p < 0.01$) in the cold seasons, with respect to spring and summer, could be due to a larger contribution of marine aerosol. The increase in the concentrations of sea salt species in the cold seasons might be attributed to local meteorological conditions, such as the occurrence of fresh wind (speed above 10 m/s) from the south with the transport of salt-enriched air mass from the sea to the land. As is well established, the sea salt species are produced at the sea surface by the bursting of air bubbles as a result of air retention induced by wind [22,23].

Table 6. Mean (min and max) concentrations of ionic components in PM_{10} at the urban-background site (NA01) ($\mu g \cdot m^{-3}$); min and max values are given in brackets.

Ionic Species	Urban-Background Site (NA01)			
	Autumn	**Winter**	**Spring**	**Summer**
F^-	0.15 (0.01–0.81)	0.050 (0.01–0.50)	0.07 (0.01–0.27)	0.08 (0.01–0.30)
Cl^-	0.91 (0.10–1.77)	1.20 (0.28–2.10)	0.57 (0.10–1.92)	0.44 (0.10–2.16)
NO_3^-	2.66 (1.00–4.10)	2.98 (0.72–5.12)	1.40 (0.85–2.26)	1.65 (0.72–2.37)
SO_4^{2-}	3.13 (1.23–4.41)	1.82 (0.82–2.97)	2.53 (0.84–3.91)	3.48 (1.25–5.75)
Na^+	1.56 (0.98–3.30)	1.64 (0.40–2.84)	0.83 (0.26–2.22)	0.80 (0.32–1.68)
NH_4^+	0.46 (0.06–1.06)	0.63 (0.09–1.30)	0.42 (0.12–0.95)	0.77 (0.25–1.52)
K^+	0.60 (0.15–1.62)	1.15 (0.12–1.60)	0.61 (0.08–1.20)	1.11 (0.80–1.76)
Mg^{2+}	0.36 (0.08–1.04)	0.48 (0.12–0.73)	0.33 (0.08–0.88)	0.20 (0.08–0.67)
Ca^{2+}	1.00 (0.36–2.19)	1.30 (0.56–2.20)	0.85 (0.39–2.39)	0.80 (0.21–2.05)

Table 7. Mean (min and max) concentrations of ionic components in PM_{10} at the urban-traffic site (NA02) ($\mu g \cdot m^{-3}$), min and max values are given in brackets.

Ionic Species	Urban-Traffic Site (NA02)			
	Autumn	**Winter**	**Spring**	**Summer**
F^-	0.83 (0.01–4.50)	0.03 (0.01–0.05)	0.05 (0.01–0.09)	0.14 (0.01–0.39)
Cl^-	1.59 (0.10–4.99)	2.21 (0.10–5.29)	0.84 (0.10–2.86)	0.53 (0.10–1.33)
NO_3^-	4.79 (1.78–8.24)	2.57 (1.58–4.69)	2.10 (1.12–4.07)	1.81 (1.19–2.40)
SO_4^{2-}	4.69 (1.64–8.59)	2.42 (1.35–4.69)	2.91 (1.01–5.92)	5.35 (1.27–8.47)
Na^+	1.82 (0.94–3.87)	2.44 (0.70–4.28)	1.13 (0.28–2.22)	0.77 (0.36–1.08)
NH_4^+	0.67 (0.06–1.91)	0.26 (0.06–0.73)	0.48 (0.06–1.40)	1.35 (0.51–2.20)
K^+	0.60 (0.33–1.36)	1.02 (0.38–1.90)	0.80 (0.33–2.05)	1.52 (0.88–2.88)
Mg^{2+}	0.40 (0.18–1.02)	0.65 (0.40–0.88)	0.33 (0.08–2.12)	0.20 (0.08–0.39)
Ca^{2+}	0.80 (0.24–2.98)	1.11 (0.81–2.01)	1.21 (0.76–2.12)	0.90 (0.44–2.85)

Ionic concentrations in Naples are comparable to those previously found in other cities, as well as to those reported for other urban sites in Europe and Asia [8–24].

Statistical software (XLSTAT 2015) [25] was used to verify the possible correlations between the different metal and ionic species in PM_{10} at the NA01 (Table 8) and NA02 (Table 9) sites.

The analysis of the single correlation coefficients showed that at both sites, there is a good correlation between Na^+ and Cl^- (0.662 for NA01 and 0.79 for NA02) and, to a lower extent, with Mg^{2+}. This result evidenced the presence of a marine contribution to the measured PM_{10} concentrations and it also supported the hypothesis of a double origin of Mg^{2+}: crustal matter and marine aerosol. The correlation between NH_4^+ and SO_4^{2-} (0.690 for NA01 and 0.660 for NA02) indicated their secondary origin. Finally, at both sites, there was a clear correlation between Fe, Al, K^+, Ca^{2+} and, to a lesser extent, Mg^{2+}, and only for NA01 was the correlation extended to Na^+. This suggested a possible common origin of these species, that is crustal mineral.

Table 8. Correlation matrices for ions analyzed in PM_{10} at the urban-background site (NA01).

	Al	Ag	Ba	Cr	Fe	Mn	Mo	Ni	Pb	Cu	V	Zn	F⁻	Cl⁻	NO₃⁻	SO₄²⁻	Na⁺	NH₄⁺	K⁺	Mg²	Ca²⁺
PM₁₀	0.25	0.48	0.30	−0.01	0.25	0.23	0.30	0.22	0.0	−0.07	0.04	−0.09	0.23	0.24	0.37	0.36	0.16	0.33	0.09	−0.25	0.09
Al	1.00	−0.11	0.08	−0.55	**0.98**	**0.60**	0.46	0.44	0.0	−0.25	−0.14	0.04	0.19	−0.11	0.30	0.20	0.36	−0.05	0.32	0.09	**0.67**
Ag		1.00	0.13	0.07	−0.11	−0.05	−0.01	−0.08	0.0	−0.05	−0.01	−0.07	−0.07	0.14	−0.01	0.05	−0.05	0.18	0.15	−0.07	−0.10
Ba			1.00	0.43	0.08	0.48	0.33	0.46	0.2	0.25	0.44	0.03	0.03	0.01	−0.11	0.18	−0.27	0.15	−0.15	−0.27	−0.09
Cr				1.00	−0.45	−0.17	−0.27	0.06	0.3	0.26	0.44	0.08	−0.23	0.24	−0.39	−0.02	−0.45	0.15	−0.42	−0.26	−0.41
Fe					1.00	0.70	0.66	0.44	0.0	−0.25	−0.14	0.04	0.19	−0.11	0.30	0.20	0.36	−0.05	0.32	0.09	**0.66**
Mn						1.00	0.32	0. 48	0.2	−0.09	0.15	0.31	0.19	−0.14	0.25	0.19	0.26	−0.12	0.24	−0.10	**0.61**
Mo							1.00	0.48	0.1	−0.18	0.00	−0.15	0.16	−0.15	0.34	0.20	0.38	−0.07	0.21	0.08	0.40
Ni								1.00	0.2	−0.02	0.32	0.03	0.06	−0.07	0.13	0.19	0.18	−0.09	−0.10	−0.16	0.18
Pb									1.0	−0.01	0.26	0.29	−0.04	−0.09	−0.07	0.09	−0.12	−0.10	−0.07	−0.18	0.14
Cu										1.00	0.12	0.03	−0.11	0.06	−0.12	−0.15	−0.23	0.04	−0.20	−0.29	−0.18
V											1.00	0.07	−0.09	−0.01	−0.17	0.15	−0.23	0.14	−0.14	−0.29	−0.14
Zn												1.00	0.05	−0.02	0.09	−0.02	0.00	−0.15	0.05	−0.11	0.00
F⁻													1.00	0.12	0.33	0.26	0.31	0.10	0.36	0.14	0.31
Cl⁻														1.00	0.15	−0.15	**0.66**	0.06	0.05	0.03	−0.07
NO₃⁻															1.00	0.33	0.30	−0.03	0.39	−0.03	0.59
SO₄²⁻																1.00	0.17	**0.69**	0.21	−0.13	0.41
Na⁺																	1.00	−0.19	0.63	0.08	**0.62**
NH₄⁺																		1.00	−0.11	−0.34	−0.01
K⁺																			1.00	0.16	**0.68**
Mg²⁺																				1.00	0.58
Ca²⁺																					1.00

Correlation is significant at the 0.05 level. * Numbers in bold are strong factor loading >0.6.

Table 9. Correlation matrices for ions analyzed in PM_{10} at the urban-traffic site (NA02).

	Al	Ag	Ba	Cr	Fe	Mn	Mo	Ni	Pb	Cu	V	Zn	F⁻	Cl⁻	NO₃⁻	SO₄²⁻	Na⁺	NH₄⁺	K⁺	Mg²	Ca²⁺
PM_{10}	**0.62**	−0.11	0.17	−0.22	**0.62**	0.32	0.48	0.11	−0.05	0.25	−0.05	0.14	0.34	0.13	0.45	0.29	0.41	0.06	0.28	0.16	0.35
Al	1.00	−0.12	0.27	−0.50	**1.00**	**0.70**	0.47	0.24	−0.04	0.26	−0.19	0.12	0.58	0.05	0.43	0.29	0.14	0.10	0.58	0.09	**0.62**
Ag		1.00	0.22	0.37	−0.12	−0.04	−0.15	0.19	0.30	0.11	0.30	0.53	−0.05	−0.08	−0.15	0.03	−0.26	0.21	0.05	−0.14	0.05
Ba			1.00	0.17	0.27	0.39	0.10	0.40	0.07	0.10	0.18	0.50	0.28	−0.29	−0.13	0.17	−0.29	0.39	0.10	−0.29	−0.08
Cr				1.00	−0.50	−0.39	−0.61	0.05	0.18	−0.14	0.46	0.27	−0.36	−0.15	−0.48	−0.03	−0.25	0.18	−0.40	−0.20	−0.35
Fe					1.00	**0.64**	0.47	0.24	−0.04	0.26	−0.19	0.12	0.58	0.05	0.43	0.29	0.14	0.10	0.58	0.09	**0.62**
Mn						1.00	0.46	0.45	0.05	**0.60**	−0.13	0.46	0.50	−0.04	0.35	0.22	0.08	0.25	0.43	−0.10	0.33
Mo							1.00	0.13	−0.07	0.19	−0.33	−0.03	0.47	0.07	0.33	0.20	0.12	−0.05	0.56	0.13	**0.47**
Ni								1.00	0.07	0.42	0.11	0.50	0.25	−0.06	−0.04	0.18	−0.12	0.26	0.12	−0.15	0.15
Pb									1.00	0.08	0.08	0.31	−0.01	−0.26	−0.15	−0.06	−0.29	0.09	−0.18	−0.21	−0.09
Cu										1.00	−0.01	0.58	0.19	0.10	0.06	0.00	0.14	0.10	0.14	−0.05	0.11
V											1.00	0.27	−0.17	−0.27	−0.33	0.24	−0.34	0.29	−0.20	−0.18	−0.23
Zn												1.00	0.08	−0.16	−0.17	0.11	−0.22	0.36	0.10	−0.27	−0.04
F⁻													1.00	0.10	0.32	0.12	0.09	−0.06	0.38	0.10	0.33
Cl⁻														1.00	0.01	−0.23	**0.80**	−0.23	0.19	0.37	0.05
NO₃⁻															1.00	0.37	0.24	−0.01	0.52	0.14	0.45
SO₄²⁻																1.00	−0.13	**0.66**	0.20	−0.05	0.34
Na⁺																	1.00	−0.22	0.12	0.31	0.07
NH₄⁺																		1.00	0.04	−0.25	0.08
K⁺																			1.00	0.16	**0.67**
Mg²⁺																				1.00	0.52
Ca²⁺																					1.00

Correlation is significant at the 0.05 level. * Numbers in bold are strong factor loading >0.6.

3.3. Carbon Species

The mean and range concentrations of the carbon species (OC, EC and IC) determined in PM_{10} at the two sites (NA01 and NA02) are shown in Tables 10 and 11, respectively.

EC is a good indicator of primary anthropogenic air pollution, while OC has a double origin; both emitted from primary emission sources and formed from chemical reactions of primary gaseous organic compounds in the atmosphere [26]. The sources of carbon aerosols can be qualitatively estimated by studying the relationship between OC and EC mass concentrations.

The OC/EC ratios (seasonal averages) at the two sites were in the range of 2.1–4.3 showing a clear prevalence of organic compared to elemental carbon species, which indicates potential secondary organic aerosol formation. The seasonal OC/EC ratios, at both sites, were comparable to those reported in the literature for other European cities [27,28].

At NA02, OC and EC concentrations showed significant seasonality ($p < 0.01$). Furthermore, OC and EC levels in the collected samples were significantly higher ($p < 0.01$) in autumn and summer. Surprisingly, in summer, the concentrations of OC were 7.3% and 4.8% higher than those registered in winter, at NA01 and NA02, respectively.

Table 10. Mean (min and max) organic carbon (OC), elemental carbon (EC) and inorganic carbon (IC) concentrations ($\mu g \cdot m^{-3}$) and concentration ratios OC/EC in PM_{10} at the urban-background site (NA01).

Carbon Species	Urban-Background Site (NA01)			
	Autumn	**Winter**	**Spring**	**Summer**
OC	3.42 (0.92–7.76)	2.97 (0.88–6.64)	2.35 (0.51–4.08)	5.02 (1.66–14.4)
EC	1.54 (0.45–3.72)	0.84 (0.43–2.04)	0.92 (0.44–1.73)	1.51 (0.81–2.88)
IC	0.41 (0.10–0.98)	0.69 (0.10–0.54)	0.37 (0.10–0.79)	0.73 (0.30–1.36)
OC/EC	2.2	3.5	2.6	3.3

Table 11. Mean (min and max) OC, EC and IC concentrations ($\mu g \cdot m^{-3}$) and concentration ratios OC/EC in PM_{10} at the urban-traffic site (NA02).

Carbon Species	Urban-Traffic Site (NA02)			
	Autumn	**Winter**	**Spring**	**Summer**
OC	7.96 (2.80–15.0)	7.80 (1.72–11.4)	5.38 (3.66–7.20)	8.77 (5.36–17.2)
EC	3.80 (1.08–6.08)	1.78 (0.64–3.13)	1.86 (0.99–3.85)	2.85 (1.57–5.63)
IC	0.46 (0.10–0.92)	1.22 (0.30–1.23)	1.02 (0.30–1.45)	0.76 (0.28–1.83)
OC/EC	2.1	4.3	2.9	3.1

3.4. Enrichment Factor

To evaluate the contribution of anthropogenic emissions to atmospheric elemental levels, the enrichment factor (EF) was calculated as Equation (1):

$$EF = (X_{PM10}/Ref_{PM10})/(X_{UCC}/Ref_{UCC}) \tag{1}$$

where X is the element under consideration both in aerosol (X_{PM10}) and upper continental crust (X_{UCC}). Metal abundances in UCC given by Wedepohl (1995) [29] were used. The analysis of the EF furnishes only qualitative information because the wide variation of the elemental concentrations of the upper crust has to be considered. In this work, Al was chosen as the reference metal (reference). Calculation has not been done for As and Cd because almost all of the samples presented concentrations under the detection limit, and this does not allow a reliable calculation of EF [30]. The results for EF in NA01 and NA02 are reported in Figure 1.
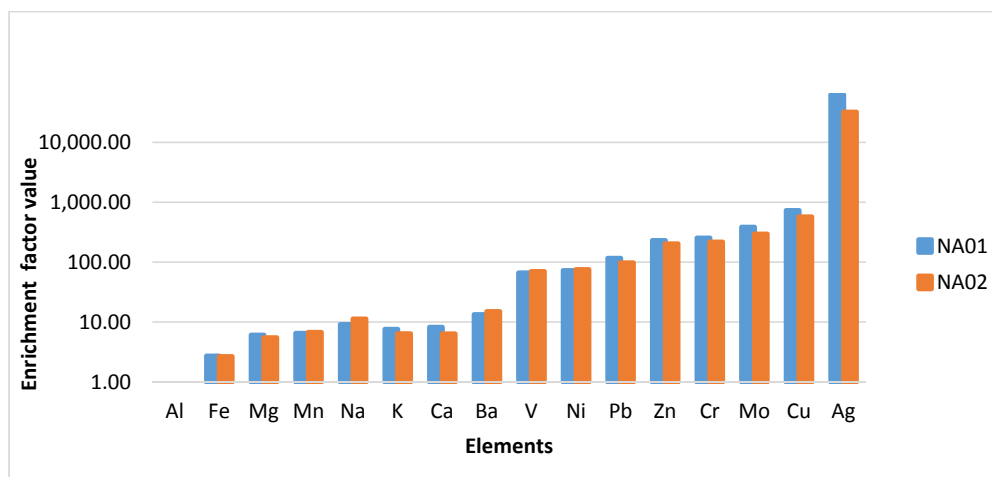
Figure 1. Crustal enrichment factor (EF) for the different elements in NA01 and NA02.

Three distinct groups existed among the metals on the basis of their EF [20]. In this work Fe, Mg, Mn, Na, K and Ca showed EF smaller then 10, indicating that these elements were not enriched and mostly derived from the crustal source; while Ba, V, Ni and Pb with EF values in the range of 10–100 suggested both natural and anthropogenic sources. Zn, Cr, Cu, Mo and Ag with average EF larger than 100 must be influenced significantly by anthropogenic sources and can be attributed to vehicular traffic (e.g., brake and tire abrasion) and industrial sources.

3.5. Reconstruction of the Chemical Composition

For reconstructing the particulate mass (mass closure), the chemical components were divided into six categories as follows: mineral dust (MD), organic matter (OM), elemental carbon (EC), sea salt (SS), secondary inorganic aerosol (SIA) and trace elements (TE). At each site, the contributions showed the differences in emission sources [31].

Mineral dust (MD) represents the sum of typical crustal materials, including Al, Si, Mg, K, Ca and Fe. Each of these species was multiplied by an appropriate factor (Equation (2)) to account for its common oxides (Al_2O_3, Fe_2O_3, CaO, MgO, K_2O) following the approach reported in the literature by several authors [8,32–34]:

$$MD = 2.2\,Al + 1.16\,Mg + 0.6\,Fe + 1.63Ca + 2.42\,Fe \tag{2}$$

K_2O was calculated as total (Fe) times 0.6. Organic matter (OM) was found by multiplying the concentration of organic carbon (OC) with a factor of 1.4 for an urban-background site and 1.3 for an urban-traffic site, as proposed by Harrison et al. [35]. The EC contribution was reported as determined by the elemental analyzer. In this study, the marine contribution (SS) (Equation (3)) was calculated, assuming that soluble Na^+ in PM_{10} samples was obtained solely from sea salt. The latter was the sum of Na^+ concentration and fractions of the concentrations of Cl^-, Mg^{2+}, K^+, Ca^{2+} and SO_4^{2-} based on the standard sea water composition and ignoring atmospheric transformation [8].

$$\text{Sea Salt} = \left[Na^+\right] + \left[ssCl^-\right] + \left[ssMg^{2+}\right] + \left[ssK^+\right] + \left[ssCa^{2+}\right] + \left[ssSO_4^{2-}\right] \tag{3}$$

Ss-Cl^- is calculated as total $[Na^+]$ times 1.8, [ss-Mg^{2+}] as total $[Na^+]$ times 0.12, [ss-K^+] as total $[Na^+]$ times 0.036, [ss-Ca^{2+}] as total $[Na^+]$ times 0.038 and [ss-SO_4^{2-}] as total $[Na^+]$ times 0.252.

Secondary inorganic aerosol (SIA) contribution was calculated as the sum of non-sea salt nss-SO_4^{2-} (calculated by subtracting ss-SO_4^{2-} from total SO_4^{2-}), NO_3^- and NH_4^+ [8,36].

Trace elements (TE) were also added to the analysis for their relevant toxicity and anthropogenic origin [37]. TE (Ba, V, Cr, Mn, Co, Ni, Cu, Zn, As, Sb, Se, Mo and Pb) represented only a small percentage (less than 1%) of the PM_{10} total mass.

The results of the chemical mass closure for PM_{10} at the two sites (NA01 and NA02) are shown as seasonal mass concentrations and relative percentage contributions in Table 12 and Figure 2.

Table 12. Seasonal mass concentration ($\mu g \cdot m^{-3}$) of PM_{10} chemical (calculated) components [a] at NA01 and NA02.

	Urban-Background Site (NA01)			
	Autumn	**Winter**	**Spring**	**Summer**
	$\mu g \cdot m^{-3}$	$\mu g \cdot m^{-3}$	$\mu g \cdot m^{-3}$	$\mu g \cdot m^{-3}$
SS	5.0 ± 1.1	5.3 ± 1.5	2.7 ± 0.8	2.6 ± 0.7
SIA	5.8 ± 0.9	5.2 ± 1.1	4.1 ± 1.2	5.2 ± 1.0
MD	4.4 ± 1.0	4.4 ± 0.6	3.4 ± 0.4	3.0 ± 1.2
OM	4.8 ± 2.0	4.2 ± 1.8	3.3 ± 1.3	7.1 ± 2.4
EC	1.5 ± 0.7	0.8 ± 0.5	0.9 ± 0.3	1.5 ± 0.4
TE	0.2 ± 0.02	0.1 ± 0.02	0.4 ± 0.02	0.3 ± 0.01
UNK	4.9 ± 1.2	5.8 ± 0.9	6.0 ± 0.6	6.3 ± 0.8
	Urban-Traffic Site (NA02)			
	Autumn	**Autumn**	**Autumn**	**Autumn**
	$\mu g \cdot m^{-3}$	$\mu g \cdot m^{-3}$	$\mu g \cdot m^{-3}$	$\mu g \cdot m^{-3}$
SS	5.8 ± 2.1	5.8 ± 2.1	5.8 ± 2.1	5.8 ± 2.1
SIA	9.7 ± 2.2	9.7 ± 2.2	9.7 ± 2.2	9.7 ± 2.2
MD	4.8 ± 1.3	4.8 ± 1.3	4.8 ± 1.3	4.8 ± 1.3
OM	10.0 ± 2.4	10.0 ± 2.4	10.0 ± 2.4	10.0 ± 2.4
EC	3.8 ± 1.3	3.8 ± 1.3	3.8 ± 1.3	3.8 ± 1.3
TE	0.3 ± 0.01	0.3 ± 0.01	0.3 ± 0.01	0.3 ± 0.01
UNK	12.6 ± 1.2	12.6 ± 1.2	12.6 ± 1.2	12.6 ± 1.2

[a] SS: sea salt; SIA: secondary inorganic aerosol; MD: mineral matter; OM: organic matter; EC: elemental carbon; TE: trace element, UNK: Unknown.
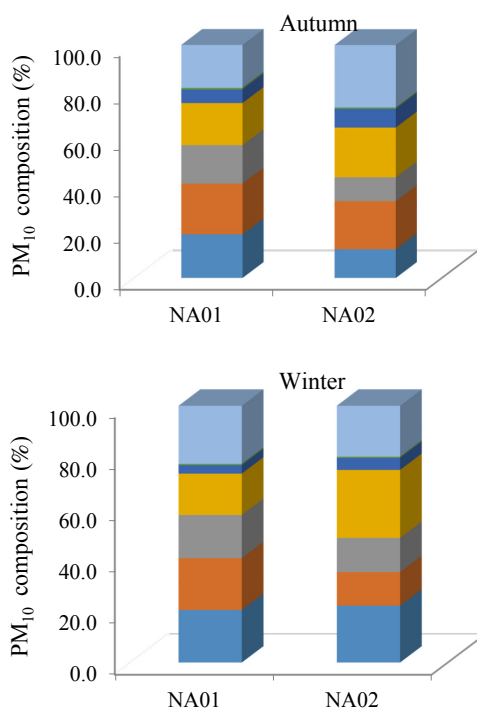

Figure 2. *Cont.*
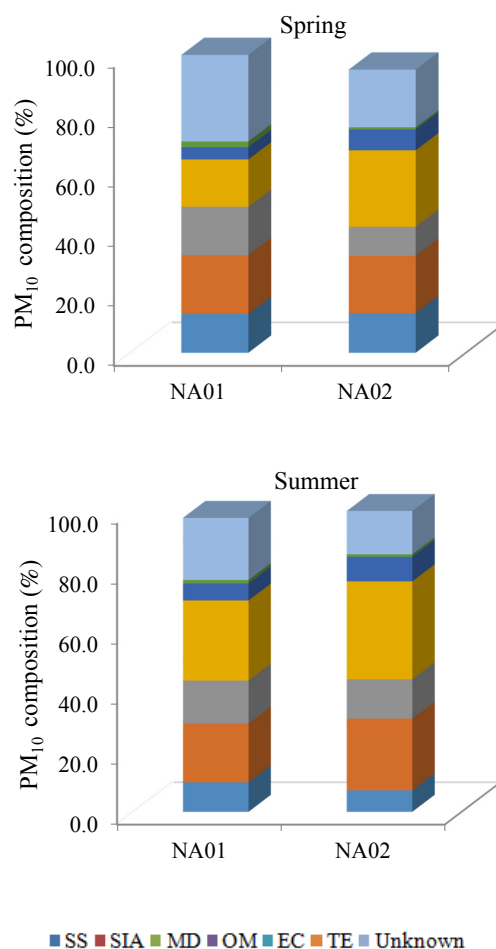
Figure 2. The percentage contribution of calculated chemical components and unidentified matter of PM$_{10}$ in sites NA01 and NA02. SS: sea salt; SIA: secondary inorganic; MD: mineral dust; OM: organic matter; EC: elemental carbon; TE: trace element.

Figure 2 shows that organic matter, secondary inorganic aerosols, mineral dust and sea salt were the main contributors to PM$_{10}$ mass concentrations at both sites.

In particular, organic matter (OM) dominated the PM$_{10}$ profiles at the NA02 site with percentage contributions in the range of 21.3%–32.6% of total PM$_{10}$ mass. The contribution of OM at both sites was higher in summer ($p < 0.01$) (32.6% and 26.7%, respectively) than in other seasons. This could be explained by the position of both sites (NA01 and NA02), which are located not far away from the harbor (about 2 and 1 km, respectively). The number of docked ships increases during the summer. In addition, the higher temperatures and lack of rain foster the process of man-triggered illegal combustion of waste, which is characteristic of the "land of fires" [38].

The mineral dust (MD) showed significant differences ($p < 0.01$) between the seasons and sites and represented a percentage between 9.8% and 16.8%. Secondary inorganic aerosol (SIA) represented a percentage between 13.1% and 23.8% of PM$_{10}$ mass. In NA02, the concentrations were significantly higher ($p < 0.01$) in autumn and summer than NA01. Due to the location of Naples, sea salt (SS) showed greater concentrations ($p < 0.01$) in the cold seasons than in the hot seasons, at both sites. In summer the percentage concentrations were lower with a value of 9.7% for NA01 and 7.1% for NA02, because the salt was dissociated into gaseous compounds more in summer than other seasons. Elemental carbon (EC) showed a percentage contribution between 3.3 and 8.1%. In NA02 during summer and autumn, the percentage contribution was higher ($p < 0.01$) than NA01. EC showed a comparable trend with OC.

On average, the calculated total mass explained about 70%–80% of the total PM_{10} mass, determined gravimetrically, for both urban-background (NA01) and traffic sites (NA02). Therefore, the unknown PM_{10} fractions mass (~20%–30%) at both sites might be attributed to the factor of conversion used for the estimation of the organic matter amount and mineral dust [39]. Figure 3 shows a linear regression of the daily reconstructed and gravimetrically-measured mass concentrations for the two sites.
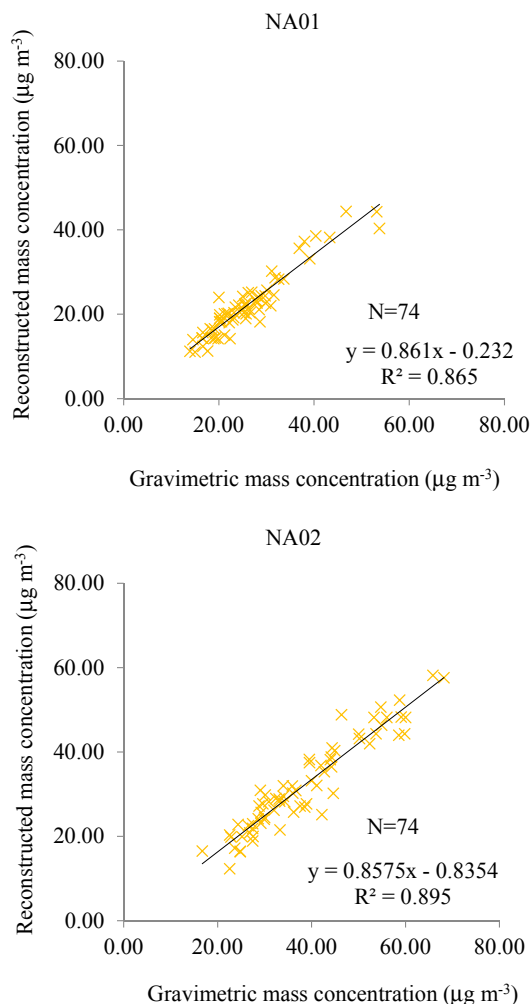
Figure 3. Linear regression of reconstructed vs. gravimetric mass concentrations.

Good correlations ($R^2 > 0.8$) were found between reconstructed mass and gravimetric mass, indicating overall good accord at both sites.

3.6. Principal Component Analysis

Principal component analysis (PCA) was used to identify the possible sources of the PM_{10} at the two sites. The main purpose of this method is to reduce the matrix of individual species into groups of data (factors). The factors can be associated by similar characteristics and therefore connected with specific sources. The varimax rotation method was used in order to identify the factor. The eigenvalue for extracted factors was more than 1.0. The number of factors is detected so that they explain the highest maximum total variance of the data. In the literature, it is recommended to use 50–200 samples subject to variable ratios (STV) of 3–20 [40].

In this study, statistical analyses were obtained using XLSTAT 2015. Factor analysis was applied to a population with the following data: N = 74, *p* = 24 and STV = 3.1. The considered components (*p*)

were: Al, Ag, Ba, Cr, Fe, Mn, Mo, Ni, Pb, Cu, V, Zn, F^-, Cl^-, NO_3^-, SO_4^{2-} Na^+, NH_4^+ K^+, Mg^{2+}, Ca^{2+}, OC, EC, IC.

Six factors were extracted as principal components (eigenvalue >1) that explained 75.7% and 79% of the variance of the data at NA01 and NA02, respectively.

The sources identified were crustal, sea salt, secondary inorganic, combustion source, road-side dust, industrial emissions and were based on the loadings of the variables in the factors (Table 13).

Table 13. PCA factor loadings for PM_{10} at NA01 and NA02. F, factor.

	NA01						NA02					
	F1	F2	F3	F4	F5	F6	F1	F2	F3	F4	F5	F6
Al	**0.777**						**0.887**					
Ag						**0.621**						**0.625**
Ba					**0.671**						0.433	
Cr					**0.749**		0.320					
Fe	**0.877**						**0.857**					
Mn	**0.676**						0.394				0.417	
Mo					0.363							
Ni	0.302										**0.685**	
Pb						**0.624**						**0.602**
Cu					**0.608**						**0.751**	
V					**0.766**						0.343	
Zn					**0.767**						**0.796**	
F^-							0.353					
Cl^-		**0.686**						**0.816**				
NO_3^-												
SO_4^{2-}			**0.690**						**0.737**			
Na^+		**0.717**						**0.738**				
NH_4^+			**0.618**						**0.659**			
K+	**0.682**						**0.682**					
Mg^{2+}	0.328				0.362			0.496				
Ca^{2+}	**0.725**						**0.790**					
OC				**0.788**						**0.753**		
IC							**0.635**					
EC				**0.704**						**0.642**		

Only loads larger than 0.3 (in absolute values) are reported. Loads larger than 0.6 (in absolute values) are in bold.

The first factor (F1) is responsible for 21% and 23% of the total variance at NA01 and NA02, respectively. F1 was designated as crustal origin by the observation of the major contribution of Al, Fe and Mn and Ca^{2+} at both sites; however, at NA02, there was an extra IC and K^+.

The second factor (F2) is responsible for 9.2% and 10% of the variance at NA01 and NA02, respectively. F2 was characterized with large amounts of Cl^- and Na^+, suggesting a sea salt origin. The third factor (F3) is responsible for 10% of the variance at NA01 and NA02, respectively, and was designated as secondary inorganic by the observation of the major contribution of NH_4^+ and SO_4^{2-}. The fourth factor (F4) is responsible for 14.5% and 16% of the variance at NA01 and NA02, respectively, and was attributed to combustion sources because of the exhibition of high loading of EC and OC. The fifth factor (F5) was attributed to road-side dust, re-suspended (from metalled roads and road pavement) by anthropogenic factors (e.g., traffic). The metals (Ba, V, Cu, Cr and, to a smaller extent, Mo and Mg^{2+}) were characteristic of NA01 and accounted for 12% of its variance, while (Ni, Cu, Zn and, to a smaller extent, Ba, Mn and V) were responsible for 14% of the variance at NA02. The sixth factor (F6) indicated a mixture of industrial emissions (Zn and Pb, for NA01, and Ag and Pb, for NA02) [41] and explained 9.0% and 6.0% of the total variance.

4. Conclusions

In this work, chemical composition, mass closure and potential emission sources of PM_{10} in Naples at the NA01 (urban-background) and NA02 (urban-traffic) sites were investigated based on

filter samples collected from October 2012–July 2013. In each season, PM_{10} concentrations were higher ($p < 0.01$) at NA02 than at NA01. The tested species were metals, ionic soluble and carbon species. Ionic soluble species considered (F^-, Cl^-, NO_3^-, SO_4^{2-}, Na^+, NH_4^+, K^+, Ca^{2+}) were about 30% of PM_{10} concentrations. At both sites, during the summer, the higher concentrations ($p < 0.01$) of SO_4^{2-} suggested an additional photochemical formation, based on meteorological conditions, but could also be related to the increase of ships docking at the port, which use fuels rich in sulfur. Otherwise, the concentrations of nitrate were lowest in summer; this could be attributed to the low thermal stability of the nitrate in the hot season; while Ca^{2+} and Mg^{2+} did not demonstrate significant seasonal variations at any of the sites, thus suggesting constant emissions throughout the year. The OC and EC levels in the collected samples were significantly higher ($p < 0.01$), particularly in autumn and summer. The metals (Al, Sb, Ag, As, Ba, Cd, Cr, Fe, Mn, Mo, Ni, Pb, Cu, Se, V and Zn) represented, on average, 3%–4% of the PM_{10} concentrations at both sites (NA01 and NA02). The enrichment factor (EF) showed a value in the range of 10–100 for Ba, V, Ni and Pb, suggesting both natural (e.g., soil and volcanic rock) and anthropogenic sources (e.g., vehicular traffic, oil burning); Zn, Cr, Cu, Mo and Ag with average EF larger than 100 must be influenced significantly by anthropogenic sources and can be attributed to vehicular traffic (e.g., brake and tire abrasion) and industrial emissions.

Mass closure allows for source reconciliation; the results of PM_{10} speciation showed that at both sites (NA01 and NA02), the PM_{10} fraction mainly was represented by organic matter (21%–33%). During summer, the contribution of OM was higher ($p < 0.01$) (32.6% and 26.7%, at NA01 and NA02, respectively) than in the other seasons. This could be explained by the position of both sites and an increase of the number of docked cruise ships. In addition, the higher temperatures and lack of rain foster the process of man-triggered illegal combustion of waste, characteristic of the "land of fires". At both sites, a good correlation ($R^2 > 0.8$) was obtained between reconstructed mass and gravimetric mass.

PCA analysis suggested the following sources: crustal, sea salt, secondary inorganic, combustion source, road-side dust and industrial emissions. The total sources explained 76% and 79% of the variance of the data at NA01 and NA02, respectively.

In conclusion, the emission sources resulted in being the same for both sites; but the location of the sites, the different distances from the sources and the presence (NA01) and absence (NA02) of vegetation proved the different concentrations of PM_{10} and especially the different compositions.

The knowledge of the source areas of the different components of PM_{10} is important in order to partly prepare for future concentrations and partly prepare for mitigating actions.

Author Contributions: Giuseppe Onorati and Beatrice Cocozziello defined the location of the sampling sites and provided samples for the analyses. Irene Saccone performed gravimetrical determinations. Francesco Frecentese, Angela Corvino and Beatrice Severino contributed to the determination of ionic species. Paola Di Vaio. and Ferdinando Fiorino determined the metal species. Anna De Marco and Elisa Magli determined carbonaceous species. Giuseppe Caliendo and Vincenzo Santagada supervised the analytical determinations. Francesco Barbato contributed to quality control. Paola Di Vaio and Maria Eleonora Soggiu contributed to the interpretation of the data and to the statistical analysis. Paola Di Vaio and Elisa Perissutti contributed to the design of the study, wrote and revised the paper.

Conflicts of Interest: The authors declare no conflict of interest.

References

1. Chan, L.Y.; Kwok, W.S. Roadside suspended particulates at heavily trafficked urban sites of Hong Kong-seasonal variation and dependence on meteorological conditions. *Atmos. Environ.* **2001**, *35*, 3177–3182. [CrossRef]

2. Grahame, T.J.; Schlesinger, RB. Cardiovascular health and particulate vehicular emissions: A critical evaluation of the evidence. *Air Q. Atmos. Health.* **2010**, *3*, 3–27. [CrossRef] [PubMed]

3. Anderson, J.O.; Thundiyil, J.G.; Stolbach, A. Clearing the air: A review of the effects of particulate matter air pollution on human health. *J. Med. Toxicol.* **2012**, *8*, 166–175. [CrossRef] [PubMed]

4. Roosli, M.; Theis, G.; Kunzli, N.; Staehelin, J.; Mathys, P.; Oglesby, L.; Camenzind, M.; Braun-Fahrlander, C. Temporal and spatial variation of the chemical composition of PM$_{10}$ at urban and rural sites in the Basel area, Switzerland. *Atmos. Environn.* **2001**, *35*, 3701–3713. [CrossRef]

5. Viana, M.; Maenhaut, W.; Chi, X.; Querol, X.; Alastuey, A. Comparative chemical mass closure of fine and coarse aerosols at two sites in south and west Europe implications for EU air pollution policies. *Atmos. Environ.* **2007**, *41*, 315–326. [CrossRef]

6. Outdoor Air Pollution. *Monographs on the Evaluation of Carcinogenic Risks to Humans*; IARC: Lyon, France, 2015.

7. Sandström, T.; Cassee, F.R.; Salonen, R.; Dybing, E. Recent outcomes in European multicentre projects on ambient particulate air pollution. *Toxicol. Appl. Pharmacol.* **2005**, *207*, 261–268. [CrossRef] [PubMed]

8. Terzi, E.; Argyropoulos, G.; Bougatioti, A.; Mihalopoulos, N.; Nikolaou, K.; Samara, C. Chemical composition and mass closure of ambient PM$_{10}$ at urban sites. *Atmos. Environ.* **2010**, *44*, 2231–2239. [CrossRef]

9. Cesari, D.; Donateo, A.; Conte, M.; Merico, E.; Giangreco, A.; Giangreco, F.; Contini, D. An inter-comparison of PM$_{2.5}$ at urban and urban background sites: Chemical characterization and source apportionment. *Atmos. Res.* **2016**, *174–175*, 106–119. [CrossRef]

10. Rocco, G.; Petitti, T.; Martucci, M.; Piccirillo, M.C.; La Rocca, A.; La Manna, C.; De Luca, G.; Morabito, A.; Chirico, A.; Franco, R.; et al. Survival after surgical treatment of lung cancer arising in the population exposed to illegal dumping of toxic waste inthe land of fires ('Terra dei Fuochi') of Southern Italy. *Anticancer Res.* **2016**, *36*, 2119–2124. [PubMed]

11. Determination of the PM$_{10}$ Fraction of Suspended Particulate Matter. EN12341 (European Standard). Available online: https://shop.austrian-standards.at/Preview.action?preview=&dokkey=67078&selectedLocale=en (accessed on 13 December 2016).

12. Standard Method for the Measurement of Pb, Cd, As and Ni in the PM$_{10}$ Fraction of Suspended Particulate Matter. EN 14902. Available online: https://www.safetyprotectionstandards.com/csn-en-14902-ambient-air-quality-standard-method-for-the-measurement-of-pb-cd-as-and-ni-in-the-pm10-fraction-of-suspended-particulate-matter/ (accessed on 13 December 2016).

13. Zappoli, S.; Andracchio, A.; Fuzzi, S.; Facchini, M.C.; Gelencser, A.; Kiss, G.; Krivacsy, Z.; Molnar, A.; Barcza, T.; Meszaros, E.; et al. Organic components and chemical mass balance of fine aerosol in different areas of Europe. *J. Aerosol. Sci.* **1998**, *29*, 731–732. [CrossRef]

14. Cachier, H.; Bremond, M.P.; Buat-Menard, P.K. Thermal separation of soot carbon. *Aerosol. Sci. Technol.* **1989**, *10*, 358–364. [CrossRef]

15. Tukey, J.W. The problem of multiple comparisons, in Time Series, 1965–1984. *Collect. Works John W Tukey Wadsworth Monterey Calif.* **1985**, *II*, 1–300.

16. Makra, L.; Ionel, I.; Csépe, Z.; Matyasovszky, I.; Lontis, N.; Popescu, F.; Sümeghy, Z. Characterizing and evaluating the role of different transport modes on urban PM10 levels in two European cities using 3D clusters of backward trajectories. *Sci. Total Environ.* **2013**, *458–460*, 36–46. [CrossRef] [PubMed]

17. Makra, L.; Puskás, J.; Matyasovszky, I.; Csépe, Z.; Lelovics, E.; Bálint, B.; Tusnády, G. Weather elements, chemical air pollutants and airborne pollen influencing asthma emergency room visits in Szeged, Hungary: Performance of two objective weather classifications. *Intern. J. Biomet.* **2015**, *59*, 1269–1289. [CrossRef] [PubMed]

18. One-way ANOVA (ANalysis Of VAriance) with Post-Hoc Tukey HSD (Honestly Significant Difference) Test Calculator for Comparing Multiple Treatments. Available online: http://astatsa.com/OneWay_Anova_with_TukeyHSD/ (accessed on 15 December 2016).

19. Almeida, S.M.; Pio, C.A.; Freitas, M.C.; Reis, M.A.; Trancoso, M.A. Source apportionment of fine and coarse particulate matter in a sub-urban area of the Western European cost. *Atmos. Environ.* **2005**, *39*, 3127–3138. [CrossRef]

20. Calvo, A.I.; Alves, C.; Castro, A.; Pont, V.; Vincente, A.M.; Fraile, R. Research on aerosol sources and chemical composition: Past, current and emerging issues. *Atmos. Environ.* **2013**, *120–121*, 1–28. [CrossRef]

21. Gholampour, A.; Nabizadeh, R.; Yunesian, M.; Naseri, S.; Taghipour, H.; Rastkari, N.; Nazmara, S.; Hossein Mahvi, A. Physicochemical Characterization of Ambient Air Particulate Matter in Tabriz, Iran. *Bull. Environ. Contam. Toxicol.* **2014**, *92*, 738–744. [CrossRef] [PubMed]

22. O'Dowd, C.D.; De Leeuw, G. Marine aerosol production: A review of the current knowledge. *R. Soc.* **2007**, *365*, 1753–1774. [CrossRef] [PubMed]

23. Cipriano, R.J.; Blanchard, D.C.; Hogan, A.W.; Lala, G.G. On the Production of Aitken Nuclei from Breaking Waves and Their Role in the Atmosphere. *Atmos. Sci. Res* **1983**, *40*, 469–479. [CrossRef]

24. Takahashi, K.; Minoura, H.; Sakamoto, K. Chemical composition of atmospheric aerosols in the general environment and around a trunk road in the Tokyo metropolitan area. *Atmos. Environ.* **2008**, *42*, 113–125. [CrossRef]

25. Huang, K.; Zhuang, G.; Lin, Y.; Fu, J.S.; Wang, Q.; Liu, T.; Zhang, R.; Jiang, Y.; Deng, C.; Fu, Q.; et al. Typical types and formation mechanisms of haze in an Eastern Asiamegacity, Shanghai. *Atmos. Chem. Phys.* **2012**, *12*, 105–124. [CrossRef]

26. Turpin, B.J.; Huntzicker, J.J. Identification of secondary organic aerosol episodes and quantitation of primary and secondary organic aerosol concentrations during SCAQS. *Atmos. Environ.* **1995**, *29*, 3527–3544. [CrossRef]

27. Salma, I.; Chi, X.; Maenhaut, W. Elemental and organic carbon in urban canyon and background environments in Budapest, Hungary. *Atmos. Environ.* **2004**, *38*, 27–36. [CrossRef]

28. Sandrini, S.; Fuzzi, S.; Piazzalunga, A.; Prati, P.; Bonasoni, P.; Cavalli, F.; Calvello, M.; Cappelletti, D.; Colombi, C.; Contini, D.; et al. Spatial and seasonal variability of carbonaceous aerosol across Italy. *Atmos. Environ.* **2014**, *99*, 587–598. [CrossRef]

29. Wedepohl, K.H. The composition of the continental crust. *Geochim. Cosmochim. Acta* **1995**, *59*, 1217–1232. [CrossRef]

30. Contini, D.; Genga, A.; Cesari, D.; Siciliano, M.; Donateo, A.; Bove, M.C.; Guascito, M.R. Characterisation and source apportionment of PM_{10} in an urban background site in Lecce. *Atmos. Res.* **2010**, *95*, 40–54. [CrossRef]

31. Marcazzan, G.M.; Vaccaro, S.; Valli, G.; Vecchi, R. Characterization of PM10 and $PM_{2.5}$ particulate matter in the ambient air of Milan (Italy). *Atmos. Environ.* **2001**, *35*, 4639–4650. [CrossRef]

32. Nava, S.; Becagli, S.; Calzolai, G.; Chiari, M.; Lucarelli, F.; Prati, P.; Traversi, R.; Udisti, R.; Valli, G.; Vecchi, R.M. Saharan dust impact in central Italy: An overview on three years elemental data records. *Atmos. Environ.* **2012**, *60*, 444–452. [CrossRef]

33. Rodríguez, S.; Querol, X.; Alastuey, A.; Viana, M.M.; Alarcón, M.; Mantilla, E.; Ruiz, C.R. Comparative PM_{10}–$PM_{2.5}$ source contribution study at rural, urban and industrial sites during PM episodes in Eastern Spain. *Sci. Total Environ.* **2014**, *328*, 95–113. [CrossRef]

34. Malm, W.C.; Schichtel, B.A.; Pitchford, M.L.; Ashbaugh, L.L.; Eldred, R.A. Spatial and monthly trends in speciated fine particle concentration in the United States. *J. Geophys. Res.* **2004**, *109*. [CrossRef]

35. Harrison, R.M.; Jones, A.M.; Lawrence, R.G. A pragmatic mass closure model for airborne particulate matter at urban background and roadside sites. *Atmos. Environ.* **2003**, *37*, 4927–4933. [CrossRef]

36. Murillo, J.H.; Roman, S.R.; Rojas Marin, J.F.; Campos, R.; Blanco, J.S.; Cardenas, G.B.; Gibson Baumgardner, D. Chemical characterization and source apportionment of PM_{10} and $PM_{2.5}$ in the metropolitan area of Costa Rica, Central America. *Atmos. Poll. Res.* **2013**, *4*, 181–190. [CrossRef]

37. Rees, S.L.; Robinson, A.L.; Khlystov, A.; Stanier, C.O.; Pandis, S.N. Mass balance closure and the federal reference method for $PM_{2.5}$ in Pittsburgh, Pennsylvania. *Atmos. Environ.* **2004**, *38*, 3305–3318. [CrossRef]

38. Mazza, A.; Piscitelli, P.; Neglia, C.; DellaRosa, G.; Iannuzzi, L. Illegal dumping of toxic waste and its effect on human health in Campania, Italy. *Int. J. Environn. Res.* **2015**, *12*, 6818–6831. [CrossRef] [PubMed]

39. Almeida, S.M.; Pio, C.A.; Freitas, M.C.; Reis, M.A.; Trancoso, M.A. Source apportionment of atmospheric urban aerosol based on weekdays/weekend: Evaluation of road re-suspended dust contribution. *Atmos. Environ.* **2006**, *40*, 2058–2067. [CrossRef]

40. De Winter, J.C.F.; Dodou, D.; Wieringa, P.A. Exploratory factor analysis with small sample sizes. *Multiv. Behav. Res.* **2009**, *44*, 147–181. [CrossRef] [PubMed]

41. Querol, X.; Minguillon, M.C.; Alastuey, A.; Monfort, E.; Mantilla, E.; Sanz, M.J.; Sanz, F.; Roig, A.; Renau, A.; Felis, C.; et al. Impact of the Implementation of PM Abatement Technology on the Ambient Air Levels of Metals in a Highly Industrialized Area. *Atmos. Environ.* **2007**, *41*, 1026–1040. [CrossRef]